

Cite this: *Phys. Chem. Chem. Phys.*, 2012, **14**, 2685–2692

www.rsc.org/pccp

Photoinduced electron transfer in covalent ruthenium–anthraquinone dyads: relative importance of driving-force, solvent polarity, and donor–bridge energy gap†

Jihane Hankache and Oliver S. Wenger*

Received 14th October 2011, Accepted 13th December 2011

DOI: 10.1039/c2cp23240e

Four rigid rod-like molecules comprised of a $\text{Ru}(\text{bpy})_3^{2+}$ ($\text{bpy} = 2,2'$ -bipyridine) photosensitizer, a 9,10-anthraquinone electron acceptor, and a molecular bridge connecting the two redox partners were synthesized and investigated by optical spectroscopic and electrochemical means. An attempt was made to assess the relative importance of driving-force, solvent polarity, and bridge variation on the rates of photoinduced electron transfer in these molecules. Expectedly, introduction of *tert*-butyl substituents in the bipyridine ligands of the ruthenium complex and a change in solvent from dichloromethane to acetonitrile lead to a significant acceleration of charge transfer rates. In dichloromethane, photoinduced electron transfer is not competitive with the inherent excited-state deactivation processes of the photosensitizer. In acetonitrile, an increase in driving-force by 0.2 eV through attachment of *tert*-butyl substituents to the bpy ancillary ligands causes an increase in electron transfer rates by an order of magnitude. Replacement of a *p*-xylene bridge by a *p*-dimethoxybenzene spacer entails an acceleration of charge transfer rates by a factor of 3.5. In the dyads from this study, the relative order of importance of individual influences on electron transfer rates is therefore as follows: solvent polarity \geq driving-force $>$ donor–bridge energy gap.

Introduction

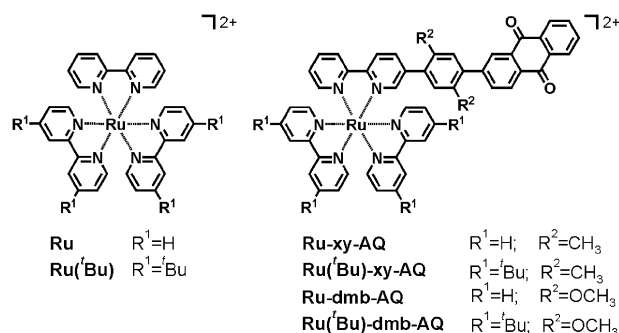
The $\text{Ru}(\text{bpy})_3^{2+}$ complex represents an extremely popular choice for investigations of photoinduced electron transfer,^{1–3} but in combination with 9,10-anthraquinone as an electron acceptor it has received rather limited attention,^{4–13} at least when compared to more potent redox partners such as viologens or tertiary amines. 9,10-Anthraquinone (AQ) is a comparatively weak oxidant,¹⁴ hence a small driving-force is usually associated with electron transfer between photoexcited $\text{Ru}(\text{bpy})_3^{2+}$ and AQ.^{15–17} The influence of driving-force and solvent variation on the rates of electron transfer in donor–bridge–acceptor molecules is nowadays fairly well understood, and the validity of theoretical models has been thoroughly tested and confirmed by numerous experimental investigations.^{1–3,18–21} The role of the molecular bridge between the donor and the acceptor has been explored in many biological and artificial systems,^{22–30} and one has obtained a fairly complete picture of what factors contribute to the overall charge transfer efficiency.

Georg-August-Universität Göttingen, Institut für Anorganische Chemie, Tammannstrasse 4, D-37077 Göttingen, Germany.
E-mail: oliver.wenger@chemie.uni-goettingen.de;

Fax: +49 (0)551 39 3373; Tel: +49 (0)551 39 19424

† Electronic supplementary information (ESI) available: Detailed synthetic protocols and product characterization data. See DOI: 10.1039/c2cp23240e

In this work we have sought to assess experimentally the relative importance of variations in driving-force, solvent polarity, and donor–bridge energy gaps in a given system. We reasoned that a donor–acceptor dyad with an inherently low driving force for electron transfer might be particularly well suited for this purpose because small variations in each of the three abovementioned parameters might have a particularly strong effect. Our choice therefore fell upon the $\text{Ru}(\text{bpy})_3^{2+}$ /anthraquinone couple, which was incorporated into rigid rod-like donor–bridge–acceptor molecules as shown in Scheme 1. As a benchmark system, a dyad comprised of a



Scheme 1 Chemical formulas of the six molecules synthesized and investigated in this work.

Ru(bpy)₃²⁺ donor (Ru), a *p*-xylene (xy) spacer, and an AQ acceptor (**Ru-xy-AQ**) was used. Driving-force variation was achieved through attachment of *tert*-butyl groups to the ancillary bpy ligands (**Ru(^tBu)-xy-AQ**), and donor–bridge energy gaps were altered through replacement of the *p*-xylene spacer by a *p*-dimethoxybenzene (dmb) unit (**Ru-dmb-AQ** and **Ru(^tBu)-dmb-AQ**). The influence of solvent polarity was explored by studying intramolecular electron transfer in these dyads in dichloromethane and acetonitrile. As reference molecules, two simple ruthenium complexes (**Ru** and **Ru(^tBu)**) were employed (Scheme 1, left).

While it is *a priori* clear how each of the individual variations of our systems (solvent exchange, *tert*-butyl group attachment to bpy ancillary ligands of the electron donor,³¹ change of the bridging spacer between the donor and acceptor) will qualitatively affect photoinduced ruthenium-to-anthraquinone electron transfer, the relative importance of these factors is more difficult to predict. The importance of donor–bridge energy matching and so-called tunneling energy gaps has long been known,^{32–34} and there have appeared numerous studies on this subject in recent years,^{35–41} including the demonstration of accelerated charge transfer in a *p*-dimethoxybenzene bridged system compared to molecules with other phenylene spacers.^{42–46} The open question is therefore not whether such acceleration will also be observed in the **Ru-dmb-AQ** and **Ru(^tBu)-dmb-AQ** dyads relative to the **Ru-xy-AQ** and **Ru(^tBu)-xy-AQ** molecules, but how important this effect will be compared to other experimental parameters that are known to affect electron transfer rates. The goal of the present study was therefore to assess and quantify the relative importance of variations in driving-force, solvent polarity, and donor–bridge energy gap for a given donor–acceptor system.

Experimental section

Synthetic procedures and product characterization data are given in the ESI.† ¹H NMR spectroscopy was performed on Bruker Avance DRX 300 and Bruker B-ACS-120 spectrometers. Electron ionization mass spectrometry (EI-MS) was performed using a Finnigan MAT8200 instrument, elemental analysis was performed on a Vario EL III CHNS analyzer from Elementar. For cyclic voltammetry, a Versastat3-100 potentiostat from Princeton Applied Research equipped with a Pt disk working electrode and a platinum counter electrode was employed. A silver wire served as a quasi-reference electrode. Ferrocene (Fc) was used as an internal reference. The supporting electrolyte was a 0.1 M solution of tetrabutylammonium hexafluorophosphate, and prior to voltage sweeps at rates of 100 mV s⁻¹, nitrogen gas was bubbled through the solutions. Optical absorption spectra were measured on a Cary 300 spectrometer from Varian. Steady-state luminescence spectra were recorded on a Fluorolog-3 instrument (FL322) from Horiba Jobin-Yvon, equipped with a TBC-07C detector from Hamamatsu. Time-resolved luminescence experiments were conducted on the same Fluorolog-3 instrument using the FL-1061PC Fluorohub for detection in TCSPC mode and a NanoLed-407 as a pulsed excitation source, or alternatively, using an LP920-KS instrument from Edinburgh Instruments. The detection system of the LP920-KS spectrometer consisted of an R928 photomultiplier and an iCCCD camera from Andor. The excitation source was a Quantel Brilliant b

laser equipped with an OPO from Opotek. Attempts to measure transient absorption were made using the same LP920-KS instrument. Before all luminescence lifetime measurements, samples were deoxygenated thoroughly by bubbling nitrogen gas through the solutions.

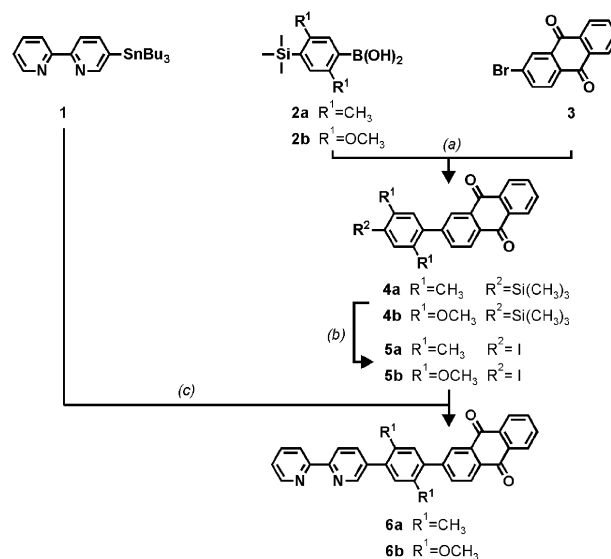
Results and discussion

Synthesis

Synthesis of the donor–bridge–acceptor molecules shown in Scheme 1 was carried out following the synthetic strategy outlined in Scheme 2. The key building blocks are 2,5-dimethyl-4-trimethylsilylphenylboronic acid (**2a**) or 2,5-dimethoxy-4-trimethylsilylphenylboronic acid (**2b**), 2-bromo-9,10-anthraquinone (**3**), and 5-(tri-*n*-butyltin)-2,2'-bipyridine (**1**). While molecule **3** is a commercially available chemical, the preparation of molecules **1**, **2a**, and **2b** has been previously described by us and others.^{47–55} Coupling of the anthraquinone acceptor to the *p*-xylene or *p*-dimethoxybenzene unit occurs conveniently under Suzuki-type conditions, and subsequent trimethylsilyl deprotection with iodine monochloride yields a compound (**5a/5b**) which can readily be coupled to the bipyridine ligand (**1**). The final step is the reaction with Ru(bpy)₂Cl₂,⁵⁶ giving the four dyads shown in Scheme 1 in overall yields ranging from 26% to 41% with respect to the 2-bromo-9,10-anthraquinone (**3**) starting material. Detailed synthetic protocols and product characterization data are given in the ESI.†

Optical absorption spectroscopy

Fig. 1 shows the optical absorption spectra of the four dyads and the two reference complexes shown in Scheme 1. The left panels (a, c) exhibit data measured in dichloromethane, the right panels (b, d) show data obtained from acetonitrile solutions. Absorption spectra of **Ru**, **Ru-xy-AQ**, and **Ru-dmb-AQ** are shown in the upper half (panels a, b) while the respective data of **Ru(^tBu)**, **Ru(^tBu)-xy-AQ**, and **Ru(^tBu)-dmb-AQ** are given in



Scheme 2 Synthetic strategy for synthesis of the bipyridine–bridge–anthraquinone ligands used in this work. (a) Pd(PPh₃)₄, toluene, water, Na₂CO₃; (b) ICl, CH₂Cl₂; (c) Pd(PPh₃)₄, *m*-xylene.

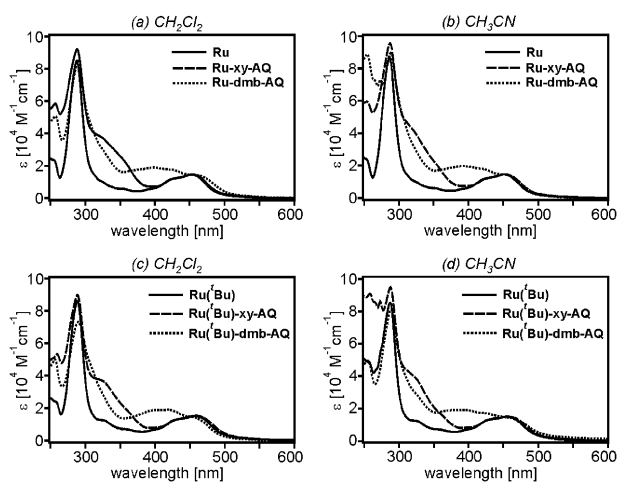


Fig. 1 Optical absorption spectra of the molecules shown in Scheme 1 in dichloromethane (a, c) and acetonitrile (b, d).

the lower half (panels c, d). The key absorption features are the same in all compounds in both solvents, namely the metal-to-ligand charge transfer (MLCT) band of the ruthenium complex centered at around 450 nm, and a bpy-localized π - π^* transition at around 290 nm.⁵⁷ All dyads exhibit a shoulder to the lower energy side of the 290 nm absorption band which may be attributed to anthraquinone-localized transitions. An interesting observation is the additional absorption between 370 and 450 nm in the two dyads with the *p*-dimethoxybenzene spacer (dotted traces): in **Ru-dmb-AQ** as well as in **Ru(^tBu)-dmb-AQ** a broad absorption with a maximum at around 400 nm is easily discernable between the MLCT band at 450 nm and the π - π^* absorption at 290 nm. This additional band is tentatively assigned to an electronic transition from the *p*-dimethoxybenzene unit to the ruthenium complex. This observation may indicate possible electronic delocalization between the ruthenium(II) chromophore and the *p*-dimethoxybenzene spacer that could be of importance for long-range electron transfer between the ruthenium and anthraquinone redox partners.

Steady-state luminescence spectroscopy

All six molecules shown in Scheme 1 are emissive in dichloromethane and acetonitrile solution after excitation into the MLCT band at 450 nm. The resulting luminescence spectra obtained in the two solvents are shown in Fig. 2, which is built up in the same way as Fig. 1: emission data obtained from dichloromethane solutions are on the left (a, c), spectra from acetonitrile solutions on the right (b, d).

In each panel, the luminescence spectra are normalized to the emission intensity of the **Ru** or **Ru(^tBu)** reference complexes. Fig. 2a shows that in dichloromethane solution **Ru** and **Ru-xy-AQ** emit with nearly equal intensities, while the luminescence of the **Ru-dmb-AQ** dyad is even somewhat stronger. From the acetonitrile data of the same compounds in Fig. 2b a different picture emerges: under these conditions the luminescence intensities decrease along the series: **Ru** > **Ru-xy-AQ** > **Ru-dmb-AQ**, and there is a factor of 4 difference between the highest (**Ru**) and lowest (**Ru-dmb-AQ**) emission intensities. This observation suggests that the change in solvent from CH₂Cl₂ to CH₃CN activates an additional nonradiative excited-state depopulation mechanism. For the

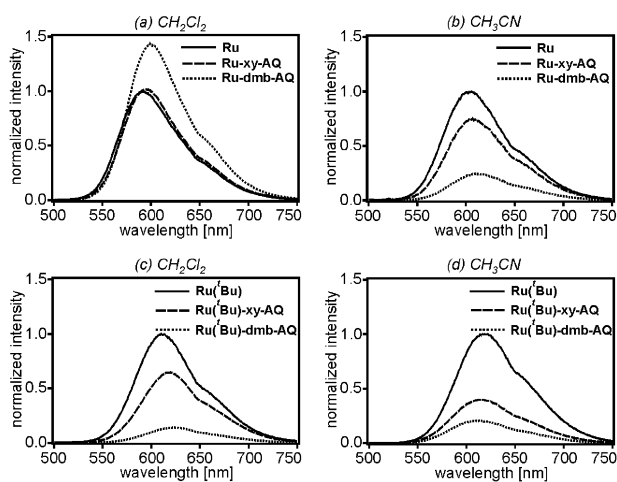


Fig. 2 Steady-state luminescence spectra of the molecules shown in Scheme 1 in dichloromethane (a, c) and acetonitrile (b, d) obtained after excitation at 450 nm.

molecules with *tert*-butyl substituted ancillary ligands, the relative luminescence intensities follow the same order given above, namely, **Ru(^tBu)** > **Ru(^tBu)-xy-AQ** > **Ru(^tBu)-dmb-AQ** (Fig. 2c and d). Thus, in the **Ru(^tBu)-xy-AQ** and **Ru(^tBu)-dmb-AQ** dyads there appears to be more efficient nonradiative excited-state deactivation than in the **Ru(^tBu)** reference complex not only in CH₃CN, but also in the less polar CH₂Cl₂ solvent.

In dichloromethane, the dyad emission band maxima are somewhat red-shifted with respect to the reference complexes. This may reflect the fact that the bpy ligand bearing the AQ-bridge moiety has its π^* LUMO at somewhat lower energy than the bpy and *tert*-butyl bpy ancillary ligands.

In principle, the emissive ³MLCT excited states of d⁶ metal diimine complexes can be depopulated efficiently by triplet-triplet energy transfer,^{58–66} provided the reaction energetics are favorable. However, for **Ru** and **Ru(^tBu)** the ³MLCT energies are 2.12 eV and 2.16 eV,⁵⁷ respectively, while the lowest triplet excited state of anthraquinone is at 2.69 eV.⁶⁷ Consequently, ruthenium-to-anthraquinone triplet-triplet energy transfer is endergonic by more than 0.5 eV and a highly improbable process. Electron transfer from photoexcited ruthenium to anthraquinone is an alternative possibility, and hence we examine the electrochemical properties of the molecules shown in Scheme 1 next.

Electrochemistry

Fig. 3 shows cyclic voltammetry data for the six molecules shown in Scheme 1 in dichloromethane (left) and acetonitrile (right) solution, measured in the presence of 0.1 M tetrabutylammonium hexafluorophosphate as a supporting electrolyte. In all voltammograms there is a wave at 0.0 V caused by the ferrocenium/ferrocene (Fc⁺/Fc) couple, which was used as an internal reference in all experiments.

Fig. 3a shows that oxidation of the **Ru** reference complex occurs at a potential of 0.97 V vs. Fc⁺/Fc in CH₂Cl₂ (solid trace), while **Ru(^tBu)** is oxidized already at 0.84 V vs. Fc⁺/Fc under the same conditions (dashed trace). The electron-donating *tert*-butyl substituents therefore facilitate metal oxidation by

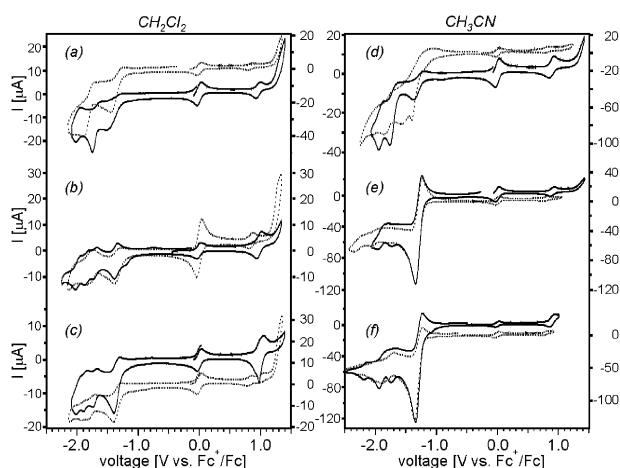


Fig. 3 Cyclic voltammograms for the six molecules shown in Scheme 1 in dichloromethane (left) and acetonitrile (right): (a, d) **Ru** (solid trace) and **Ru(Bu)** (dotted trace); (b, e) **Ru-xy-AQ** (solid) and **Ru(Bu)-xy-AQ** (dotted); (c, f) **Ru-dmb-AQ** (solid) and **Ru(Bu)-dmb-AQ** (dotted).

130 mV, an effect which is well known and which can also be observed in the *p*-xylene (Fig. 3b) and *p*-dimethoxybenzene (Fig. 3c) bridged dyads.⁵⁷ Likewise, the same effect is observed in acetonitrile for all molecules, albeit in somewhat attenuated form. For convenience, all electrochemical potentials for ruthenium oxidation ($E(\text{Ru}^{\text{II/III}})$) extracted from Fig. 3 have been summarized in the third column of Table 1. The data show that the **Ru** unit with unsubstituted ancillary bpy ligands is easier to oxidize by ~ 100 mV in acetonitrile compared to dichloromethane, while in the **Ru(Bu)**-based systems the difference between solvents only amounts to roughly 50 mV.

For estimation of the driving force for photoinduced electron transfer from ruthenium to anthraquinone, the electrochemical potential for one-electron reduction of the anthraquinone moiety ($E(\text{AQ}^{0/-})$) is particularly relevant. From literature data, we expect this reduction process to occur near -1.3 V vs. Fc^+/Fc , and we indeed observe prominent reduction waves at this potential in Fig. 3b, c, e and f. Inspection of the voltammograms of the pure reference complexes in Fig. 3a (**Ru**) and Fig. 3d

Table 1 Electrochemical potentials (E) for oxidation of $\text{Ru}(\text{II})$ to $\text{Ru}(\text{III})$ and for reduction of AQ^0 to AQ^- in volts versus Fc^+/Fc ; free energy (ΔG_{ET}) associated with photoinduced electron transfer from ruthenium to anthraquinone (calculated with eqn (1) and the parameters given in the text)

Compound	Solvent	$E(\text{Ru}^{\text{II/III}})$	$E(\text{AQ}^{0/-})$	$\Delta G_{\text{ET}}/\text{eV}$
Ru	CH_2Cl_2	0.97		
Ru	CH_3CN	0.88		
Ru-xy-AQ	CH_2Cl_2	0.98	-1.35	0.09
Ru-xy-AQ	CH_3CN	0.90	-1.29	0.04
Ru-dmb-AQ	CH_2Cl_2	1.00	-1.34	0.10
Ru-dmb-AQ	CH_3CN	0.90	-1.27	0.02
Ru(Bu)	CH_2Cl_2	0.84		
Ru(Bu)	CH_3CN	0.80		
Ru(Bu)-xy-AQ	CH_2Cl_2	0.83	-1.33	-0.12
Ru(Bu)-xy-AQ	CH_3CN	0.79	-1.29	-0.11
Ru(Bu)-dmb-AQ	CH_2Cl_2	0.83	-1.33	-0.12
Ru(Bu)-dmb-AQ	CH_3CN	0.79	-1.29	-0.11

(**Ru(Bu)**) reveals that reduction processes associated with the ruthenium complexes occur at a similar potential, indeed, these are the well known ligand-based reductions of $\text{Ru}(\alpha\text{-diimine})_3^{2+}$ -type complexes.⁵⁷ Thus, in the voltammograms of the dyads (Fig. 3b, c, e and f) at potentials below -1.2 V vs. Fc^+/Fc there are overlapping waves due to bpy-based and AQ-localized reductions. However, the shapes of the most prominent reduction waves at -1.3 V vs. Fc^+/Fc , particularly in CH_3CN , are reminiscent of the voltammogram reported for isolated 9,10-anthraquinone and are therefore attributed to an AQ-localized reduction process.¹⁴ All $E(\text{AQ}^{0/-})$ -values are summarized in the fourth column of Table 1. Nearly the same reduction potential is found for all four dyads shown in Scheme 1, irrespective of whether CH_2Cl_2 or CH_3CN is used as a solvent.

Thermodynamics of photoinduced electron transfer

Based on the electrochemical data from the preceding paragraph, we are now in a position to estimate the driving force for electron transfer (ΔG_{ET}) between photoexcited ruthenium and anthraquinone in the four dyads shown in Scheme 1. Eqn (1) is commonly used for the purpose of estimating driving forces for photoinduced electron transfer.^{1,37,68}

$$\Delta G_{\text{ET}} = e \cdot (E_{\text{ox}} - E_{\text{red}}) - E_{00} - e^2 / (4\pi\epsilon_0\epsilon_s R_{\text{DA}}) \quad (1)$$

In eqn (1), E_{ox} and E_{red} are the electrochemical potentials for ruthenium oxidation ($E(\text{Ru}^{\text{II/III}})$) and anthraquinone reduction ($E(\text{AQ}^{0/-})$), respectively, while E_{00} is the energy of the photoactive $^3\text{MLCT}$ state of the ruthenium complex. ϵ_0 is the vacuum permittivity, and ϵ_s stands for the dielectric constant of the solvent (dichloromethane: 8.93, acetonitrile: 35.94).⁶⁹ r represents the average Born radius of the two redox partners (assumed to be 4.5 \AA), and R_{DA} is the center-to-center donor-acceptor distance (13.3 \AA). Using the redox potentials from Table 1 and a $^3\text{MLCT}$ energy of 2.12 eV for the unsubstituted **Ru** complex, we find that for **Ru-xy-AQ** and **Ru-dmb-AQ** photoinduced electron transfer is endergonic by 0.09 eV/0.10 eV in dichloromethane, while in acetonitrile $\Delta G_{\text{ET}} = 0.04$ eV/0.02 eV for the same two dyads (last column of Table 1). As expected, photoinduced electron transfer is less endergonic in the more polar CH_3CN solvent, partly due to the fact that ruthenium oxidation occurs more readily under these conditions (see the third column of Table 1 and the preceding paragraph).

The differences in ΔG_{ET} between solvents are likely responsible for the discrepancies in luminescence behavior observed for the **Ru-xy-AQ/Ru-dmb-AQ** dyads in dichloromethane (Fig. 2a) and acetonitrile (Fig. 2b). In CH_2Cl_2 , $\Delta G_{\text{ET}} \approx 0.1$ eV and hence excited-state deactivation by electron transfer is inefficient, and the **Ru**, **Ru-xy-AQ**, and **Ru-dmb-AQ** luminescence intensities are all about equal (Fig. 2a). In CH_3CN , $\Delta G_{\text{ET}} < 0.1$ eV, leading to noticeable luminescence quenching in the dyads with respect to the **Ru** reference complex as a consequence of intramolecular photoinduced electron transfer. It appears plausible that the normalized luminescence intensities in this case (Fig. 2b) reflect the relative electron transfer efficiencies, but this aspect will be further examined below.

As far as the dyads with the **Ru(Bu)** photosensitizer are concerned, the change in solvent from CH_2Cl_2 to CH_3CN has

qualitatively the same influence as on the dyads with the ordinary **Ru** complex without *tert*-butyl groups: photoinduced electron transfer in **Ru**(**Bu**)-*xy*-AQ/**Ru**(**Bu**)-*dmb*-AQ becomes more favorable in acetonitrile (Table 1, fifth column). Excited-state quenching by electron transfer is efficient already in CH₂Cl₂, hence the emission of **Ru**(**Bu**)-*xy*-AQ and **Ru**(**Bu**)-*dmb*-AQ is weaker than that of **Ru**(**Bu**) already in dichloromethane (Fig. 2c) and not only in acetonitrile (Fig. 2d).³¹

Kinetics for photoinduced electron transfer

With the thermodynamics for photoinduced electron transfer in all four dyads at hand, we may now turn to the kinetics of this excited-state deactivation process. Time-resolved luminescence and transient absorption spectroscopy are among the two most widely used experimental techniques for exploration of the dynamics of electron transfers occurring from excited states. In the dyads shown in Scheme 1, photoinduced electron transfer is expected to produce an oxidized ruthenium complex and a reduced anthraquinone moiety, both of which have clearly identifiable absorptions in the visible spectral range. However, all our attempts to detect oxidized ruthenium (*e.g.*, by a bleach in transient absorption at around 450 nm) or reduced anthraquinone (*e.g.*, by searching positive transient absorption signals at 390 nm or 550 nm)^{17,70} by nanosecond transient absorption spectroscopy have failed, presumably due to rapid disappearance of the respective photoproducts by thermal electron transfer in the opposite sense. Indeed, this is not an uncommon problem in investigations of photoinduced electron transfer, including prior studies of ruthenium–benzoquinone dyads.⁷¹ Thus, our kinetic investigations are limited to time-resolved luminescence experiments. We recall that excited-state quenching by triplet–triplet energy transfer could be ruled out based on energetic grounds (see above).

Fig. 4 shows the luminescence decays of the six molecules shown in Scheme 1 detected at 600 nm after pulsed excitation at 407 nm or at 450 nm. The left panels (a, c) show data measured in dichloromethane, while the right panels (b, d) exhibit lifetimes determined in acetonitrile. With the exception of **Ru**(**Bu**)-*xy*-AQ and **Ru**(**Bu**)-*dmb*-AQ in acetonitrile (Fig. 4d), all emission decays are single exponential, and fits to the experimental data in Fig. 4 yield the lifetime values (τ) given in Table 2. Inspection of panels (a) and (c) in Fig. 4 reveals that all six molecules shown in Scheme 1 exhibit luminescence lifetimes longer than 500 ns in deoxygenated dichloromethane solution. For the molecules based on the **Ru** photosensitizer, the relative magnitude of the emission lifetimes reflects the relative luminescence intensities in Fig. 2a: **Ru** has the shortest lifetime (535 ns) and the weakest intensity, while **Ru**-*dmb*-AQ has the longest lifetime (1865 ns) and strongest intensity; **Ru**-*xy*-AQ is between the two, both regarding the lifetime (696 ns) and emission intensity. In acetonitrile, the strongest emitter (Fig. 2b) is the isolated **Ru** complex exhibiting a luminescence lifetime of 866 ns, **Ru**-*dmb*-AQ shows the weakest emission and shortest lifetime (124 ns), while **Ru**-*xy*-AQ is in between both regarding the intensity and lifetime (300 ns). The changes in emission intensity and luminescence lifetime upon solvent replacement from CH₂Cl₂ to CH₃CN are both consistent with an increased

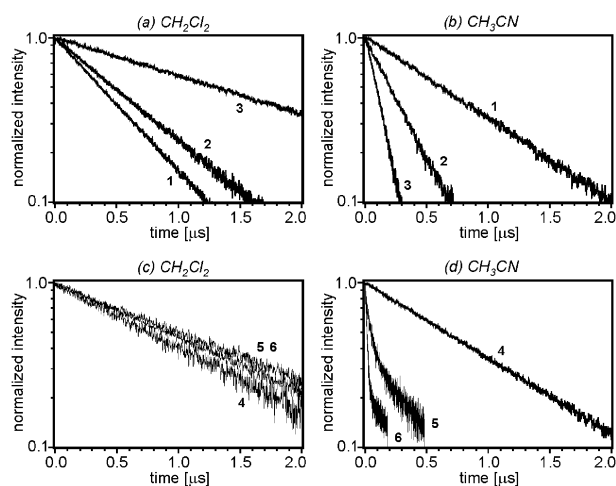


Fig. 4 Luminescence decays of the molecules shown in Scheme 1 in CH₂Cl₂ (a, c) and CH₃CN (b, d) measured after pulsed excitation at 407 nm or 450 nm. Labels are as follows: 1: **Ru**, 2: **Ru**-*xy*-AQ, 3: **Ru**-*dmb*-AQ, 4: **Ru**(**Bu**), 5: **Ru**(**Bu**)-*xy*-AQ, 6: **Ru**(**Bu**)-*dmb*-AQ.

Table 2 Luminescence lifetimes (τ) and excited-state quenching rate constants (k_Q) in deoxygenated solution. Excitation occurred at 407 nm or 450 nm, detection was at 600 nm. k_Q -values were calculated using eqn (2) and reflect rate constants for photoinduced ruthenium-to-anthraquinone electron transfer. 1: **Ru**, 2: **Ru**-*xy*-AQ, 3: **Ru**-*dmb*-AQ, 4: **Ru**(**Bu**), 5: **Ru**(**Bu**)-*xy*-AQ, 6: **Ru**(**Bu**)-*dmb*-AQ

Solvent	τ /ns	τ /ns	τ /ns	k_Q/s^{-1}	k_Q/s^{-1}
	1	2	3	2	3
CH ₂ Cl ₂	535	696	1865	$< 1.4 \times 10^6$	$< 5.4 \times 10^5$
CH ₃ CN	866	300	124	$(2.2 \pm 0.2) \times 10^6$	$(6.9 \pm 0.5) \times 10^6$
Solvent	τ /ns	τ /ns	τ /ns	k_Q/s^{-1}	k_Q/s^{-1}
	4	5	6	5	6
CH ₂ Cl ₂	1231	1394	1510	$< 7.2 \times 10^5$	$< 6.6 \times 10^5$
CH ₃ CN	947	47	14	$(2.0 \pm 0.1) \times 10^7$	$(7.0 \pm 0.4) \times 10^7$
		(50%)	(67%)		
		950	950		
		(50%)	(33%)		

efficiency of photoinduced ruthenium-to-anthraquinone electron transfer as a result of increased driving-force (ΔG_{ET} , Table 1).

In the absence of transient absorption data which could provide direct kinetic information regarding the build-up of electron transfer photoproducts, it is common to use eqn (2) to determine excited-state quenching rate constants (k_Q).^{1,66}

$$k_Q = \tau_{\text{dyad}}^{-1} - \tau_{\text{ref}}^{-1} \quad (2)$$

In eqn (2), τ_{dyad} is the lifetime of the ruthenium–bridge–anthraquinone dyad, and τ_{ref} is the luminescence lifetime of a suitable reference complex. It is customary to use complexes such as **Ru** and **Ru**(**Bu**) as reference compounds. For the **Ru**-*xy*-AQ and **Ru**-*dmb*-AQ dyads this procedure results in k_Q -values of $(2.2 \pm 0.2) \times 10^6 \text{ s}^{-1}$ and $(6.9 \pm 0.5) \times 10^6 \text{ s}^{-1}$ in acetonitrile. For dichloromethane solution, this procedure is not applicable because there is no significant luminescence quenching or lifetime shortening in these two particular dyads with respect to the reference complex. Therefore, instead of applying eqn (2) to the dichloromethane data, we simply

estimate an upper limit for k_Q of **Ru-xy-AQ** and **Ru-dmb-AQ** in CH_2Cl_2 in the following way: in the (unrealistic) limiting case in which excited-state deactivation would occur entirely by Ru-to-AQ electron transfer, $k_Q = \tau_{\text{dyad}}^{-1}$. In the presence of other excited-state deactivation pathways (e.g., luminescence, multiphonon relaxation), $k_Q < \tau_{\text{dyad}}^{-1}$, hence by using the approximation $k_Q \approx \tau_{\text{dyad}}^{-1}$ one can estimate the upper limit of k_Q for **Ru-xy-AQ** and **Ru-dmb-AQ** in CH_2Cl_2 even without having a suitable reference point at disposition.

In the dyads with the **Ru(Bu)** photosensitizer, the time-resolved luminescence data in Fig. 4c provide no evidence for significant excited-state quenching in dichloromethane, and one is forced to conclude that the electron transfer rate constant is below $7.2 \times 10^5 \text{ s}^{-1}$ for **Ru(Bu)-xy-AQ** and below $6.6 \times 10^5 \text{ s}^{-1}$ in **Ru(Bu)-dmb-AQ** in CH_2Cl_2 . In deoxygenated acetonitrile (Fig. 4d), $\tau = 947 \text{ ns}$ for **Ru(Bu)**, while the **Ru(Bu)-xy-AQ** and **Ru(Bu)-dmb-AQ** dyads both exhibit biexponential decays, with a fast decay component yielding lifetimes of 47 ns (xy system) and 14 ns (dmb system), respectively, and a second decay component which is markedly slower and which can be fitted to a lifetime of $\sim 950 \text{ ns}$ in both cases. This slower component is attributed to emission of a **Ru(Bu)** impurity present in the **Ru(Bu)-xy-AQ** and **Ru(Bu)-dmb-AQ** samples. By standard analytical methods (NMR, elemental analysis) this impurity is not detectable (see the ESI[†]), but given the fast luminescence decay of **Ru(Bu)-xy-AQ** (47 ns) and **Ru(Bu)-dmb-AQ** (14 ns) in acetonitrile (Table 2), even minute amounts of comparatively strongly emissive impurities now become noticeable. The same effect may explain the observation of nearly identical emission intensities for the **Ru(Bu)**-based dyads in CH_2Cl_2 (Fig. 2c) and CH_3CN (Fig. 2d). Given the much shorter lifetimes in acetonitrile than in dichloromethane, the inherent dyad emission intensities are expected to be significantly lower in CH_3CN , and it is likely that a **Ru(Bu)** impurity contributes substantially to the dyad emissions in Fig. 2d. Be that as it may, given the long **Ru(Bu)-xy-AQ/Ru(Bu)-dmb-AQ** lifetimes in CH_2Cl_2 compared to the **Ru(Bu)** reference complex, application of eqn (2) makes sense only for acetonitrile solvent in which substantial lifetime shortening in the dyads is observed. In this case, rate constants of $(2.0 \pm 0.1) \times 10^7 \text{ s}^{-1}$ and $(7.0 \pm 0.4) \times 10^7 \text{ s}^{-1}$ are obtained for the xylene- and dimethoxybenzene-bridged systems, respectively (Table 2).

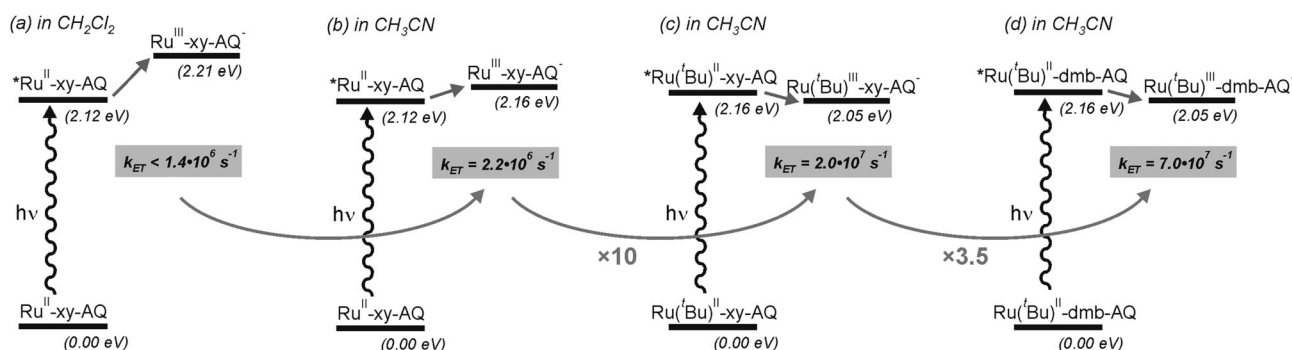
Curiously, the emission lifetimes of the **Ru-xy-AQ** and **Ru-dmb-AQ** dyads in CH_2Cl_2 are significantly longer than

the luminescence lifetime of the Ru reference complex under identical conditions. This observation, together with the finding of (slightly) increasing emission intensities along the series: **Ru** < **Ru-xy-AQ** < **Ru-dmb-AQ** in CH_2Cl_2 (Fig. 2a), indicates that nonradiative relaxation becomes less efficient along this series of compounds. The origin of this effect is not understood.

Summary and conclusions

The key findings from this work are summarized in Scheme 3. From the k_Q -values in Table 2 we learn that the change in solvent from CH_2Cl_2 (Scheme 3a) to CH_3CN (Scheme 3b) increases charge transfer rates to the extent that electron transfer becomes a competitive excited-state deactivation pathway. Introduction of electron-donating *tert*-butyl substituents in the bpy ancillary ligands and the associated increase in $-\Delta G_{\text{ET}}$ by $\sim 0.2 \text{ eV}$ (Table 1) entail an acceleration by an order of magnitude (e.g., from $2.2 \times 10^6 \text{ s}^{-1}$ for **Ru-xy-AQ** to $2.0 \times 10^7 \text{ s}^{-1}$ for **Ru(Bu)-xy-AQ**, Scheme 3c). Finally, replacement of the *p*-xylene spacer by a *p*-dimethoxybenzene unit leads to an increase in electron transfer rates by a factor of 3.5 (e.g., from $2.0 \times 10^7 \text{ s}^{-1}$ in **Ru(Bu)-xy-AQ** to $7.0 \times 10^7 \text{ s}^{-1}$ in **Ru(Bu)-dmb-AQ**, Scheme 3d). Thus, the relative importance of the three effects decreases along the series: solvent polarity \geq *tert*-butyl substitution > bridge modulation.

The influence of the molecular bridge on electron transfer rates is relatively small in the present case. The *p*-dimethoxybenzene molecule is oxidized much more easily than *p*-xylene, and therefore it is prone to mediating charge transfer predominantly *via* a hole transfer mechanism, as previously demonstrated for hole transfers originating from photogenerated $\text{Ru}(\text{bpy})_3^{3+}$ complexes.^{72,73} In the present case, we are dealing with excited-state electron transfer from ruthenium(II) to anthraquinone, or equivalently, hole transfer from anthraquinone to photoexcited ruthenium(II). Based on the electrochemical potential for one-electron oxidation of *p*-dimethoxybenzene (1.1 V vs. Fc^+/Fc)^{74,75} and the reduction potential of anthraquinone (-1.3 V vs. Fc^+/Fc , Table 2), hole injection from anthraquinone to *p*-dimethoxybenzene is energetically uphill by 2.4 eV. In the case of the *p*-xylene dyads, the respective injection barrier amounts to more than 3.0 eV, based on an oxidation potential $> 1.7 \text{ V}$ vs. Fc^+/Fc for *p*-xylene.⁷⁴ Given the fact that the donor-bridge energy gap decreases by only about 20% between the xylene- and dimethoxybenzene-bridged dyads,



Scheme 3 Energetics and kinetics of photoinduced electron transfer as a function of solvent, driving-force, and bridge modulation.

the experimentally observed acceleration of charge transfer rates by a factor of 3.5 is remarkable.

The bottom line is that in our dyads a 0.2 eV increase in driving-force has a stronger influence on charge transfer rates than the 0.6 eV decrease in the donor–bridge energy gap associated with the replacement of a *p*-xylene spacer by a *p*-dimethoxybenzene unit. However, this is because the absolute magnitude of the barrier for hole injection into the bridge is large for the particular systems investigated here. It is conceivable that for other donor–bridge–acceptor combinations with inherently smaller injection barriers, variations in donor–bridge energy gaps outweigh the effect of small driving-force changes—even in the tunneling regime, before hopping processes become energetically viable.

Acknowledgements

This work was supported by the Swiss National Science Foundation through grant number 200021-117578 and the Deutsche Forschungsgemeinschaft through grant number INST 186/872-1.

Notes and references

- V. Balzani, *Electron transfer in chemistry*, VCH Wiley, Weinheim, 2001.
- A. Juris, V. Balzani, F. Barigelletti, S. Campagna, P. Belser and A. Von Zelewsky, *Coord. Chem. Rev.*, 1988, **84**, 85.
- O. S. Wenger, *Coord. Chem. Rev.*, 2009, **253**, 1439.
- C. J. da Cunha, E. S. Dodsworth, M. A. Monteiro and A. B. P. Lever, *Inorg. Chem.*, 1999, **38**, 5399.
- R. Frank, G. Greiner and H. Rau, *Phys. Chem. Chem. Phys.*, 1999, **1**, 3481.
- R. Frank and H. Rau, *Helv. Chim. Acta*, 2001, **84**, 3837.
- D. G. McCafferty, D. A. Friesen, E. Danielson, C. G. Wall, M. J. Saderholm, B. W. Erickson and T. J. Meyer, *Proc. Natl. Acad. Sci. U. S. A.*, 1996, **93**, 8200.
- D. R. Striplin, S. Y. Reece, D. G. McCafferty, C. G. Wall, D. A. Friesen, B. W. Erickson and T. J. Meyer, *J. Am. Chem. Soc.*, 2004, **126**, 5282.
- F. Vögtle, M. Plevoets, M. Nieger, G. C. Azzellini, A. Credi, L. De Cola, V. De Marchis, M. Venturi and V. Balzani, *J. Am. Chem. Soc.*, 1999, **121**, 6290.
- K. Sumi, M. Furue and S. Nozakura, *Photochem. Photobiol.*, 1985, **42**, 485.
- J. Otsuki, H. Ogawa, N. Okuda, K. Araki and M. Seno, *Bull. Chem. Soc. Jpn.*, 1997, **70**, 2077.
- L. Mishra, C. S. Choi and K. Araki, *Chem. Lett.*, 1997, 447.
- Y. Pellegrin, R. J. Forster and T. E. Keyes, *Inorg. Chim. Acta*, 2009, **362**, 1715.
- A. Babaei, P. A. Connor, A. J. McQuillan and S. Umaphathy, *J. Chem. Educ.*, 1997, **74**, 1200.
- S. L. Mecklenburg, D. G. McCafferty, J. R. Schoonover, B. M. Peek, B. W. Erickson and T. J. Meyer, *Inorg. Chem.*, 1994, **33**, 2974.
- K. A. Opperman, S. L. Mecklenburg and T. J. Meyer, *Inorg. Chem.*, 1994, **33**, 5295.
- J. Hankache and O. S. Wenger, *Chem. Commun.*, 2011, **47**, 10145.
- M. R. Wasielewski, *Chem. Rev.*, 1992, **92**, 435.
- P. Y. Chen and T. J. Meyer, *Chem. Rev.*, 1998, **98**, 1439.
- P. F. Barbara, T. J. Meyer and M. A. Ratner, *J. Phys. Chem.*, 1996, **100**, 13148.
- H. B. Gray and J. R. Winkler, *Proc. Natl. Acad. Sci. U. S. A.*, 2005, **102**, 3534.
- H. B. Gray and J. R. Winkler, *Annu. Rev. Biochem.*, 1996, **65**, 537.
- J. R. Winkler and H. B. Gray, *Chem. Rev.*, 1992, **92**, 369.
- B. Giese, *Annu. Rev. Biochem.*, 2002, **71**, 51.
- M. Cordes and B. Giese, *Chem. Soc. Rev.*, 2009, **38**, 892.
- B. Albinsson, M. P. Eng, K. Pettersson and M. U. Winters, *Phys. Chem. Chem. Phys.*, 2007, **9**, 5847.
- B. Albinsson and J. Mårtensson, *J. Photochem. Photobiol., C*, 2008, **9**, 138.
- W. R. Browne, N. M. O'Boyle, J. J. McGarvey and J. G. Vos, *Chem. Soc. Rev.*, 2005, **34**, 641.
- F. Scandola, M. T. Indelli, C. Chiorboli and C. A. Bignozzi, *Top. Curr. Chem.*, 1990, **158**, 73.
- A. C. Benniston and A. Harriman, *Chem. Soc. Rev.*, 2006, **35**, 169.
- H. A. Meylemans, C. F. Lei and N. H. Damrauer, *Inorg. Chem.*, 2008, **47**, 4060.
- H. M. McConnell, *J. Chem. Phys.*, 1961, **35**, 508.
- M. N. Paddon-Row, *Acc. Chem. Res.*, 1994, **27**, 18.
- M. N. Paddon-Row, A. M. Oliver, J. M. Warman, K. J. Smit, M. P. Dehaas, H. Oevering and J. W. Verhoeven, *J. Phys. Chem.*, 1988, **92**, 6958.
- M. P. Eng and B. Albinsson, *Angew. Chem., Int. Ed.*, 2006, **45**, 5626.
- M. P. Eng and B. Albinsson, *Chem. Phys.*, 2009, **357**, 132.
- K. Kilsä, J. Kajanus, A. N. Macpherson, J. Mårtensson and B. Albinsson, *J. Am. Chem. Soc.*, 2001, **123**, 3069.
- J. Wiberg, L. J. Guo, K. Pettersson, D. Nilsson, T. Ljungdahl, J. Mårtensson and B. Albinsson, *J. Am. Chem. Soc.*, 2007, **129**, 155.
- K. Pettersson, J. Wiberg, T. Ljungdahl, J. Mårtensson and B. Albinsson, *J. Phys. Chem. A*, 2006, **110**, 319.
- O. S. Wenger, *Acc. Chem. Res.*, 2011, **44**, 25.
- O. S. Wenger, *Chem. Soc. Rev.*, 2011, **40**, 3538.
- S. E. Miller, A. S. Lukas, E. Marsh, P. Bushard and M. R. Wasielewski, *J. Am. Chem. Soc.*, 2000, **122**, 7802.
- C. Lambert, G. Nöll and J. Schelter, *Nat. Mater.*, 2002, **1**, 69.
- D. Hanss, M. E. Walther and O. S. Wenger, *Chem. Commun.*, 2010, **46**, 7034.
- M. E. Walther and O. S. Wenger, *ChemPhysChem*, 2009, **10**, 1203.
- J. Hankache and O. S. Wenger, *Chem. Rev.*, 2011, **111**, 5138.
- N. Belfrek, C. Dietrich-Buchecker and J.-P. Sauvage, *Tetrahedron Lett.*, 2001, **42**, 2779.
- V. Hensel and A. D. Schlüter, *Liebigs Ann.*, 1997, 303.
- V. Hensel, K. Lutzow, J. Jacob, K. Gessler, W. Saenger and A. D. Schlüter, *Angew. Chem., Int. Ed.*, 1997, **36**, 2654.
- M. E. Walther and O. S. Wenger, *Inorg. Chem.*, 2011, **50**, 10901.
- D. Hanss, J. C. Freys, G. Bernardinelli and O. S. Wenger, *Eur. J. Inorg. Chem.*, 2009, 4850.
- A. Bouillon, A. S. Voisin, A. Robic, J. C. Lancelot, V. Collot and S. Rault, *J. Org. Chem.*, 2003, **68**, 10178.
- M. S. Jensen, R. S. Hoerrner, W. J. Li, D. P. Nelson, G. J. Javadi, P. G. Dormer, D. W. Cai and R. D. Larsen, *J. Org. Chem.*, 2005, **70**, 6034.
- D. Hanss and O. S. Wenger, *Inorg. Chem.*, 2008, **47**, 9081.
- D. Hanss and O. S. Wenger, *Inorg. Chem.*, 2009, **48**, 671.
- B. P. Sullivan, D. J. Salmon and T. J. Meyer, *Inorg. Chem.*, 1978, **17**, 3334.
- D. M. Roundhill, *Photochemistry and Photophysics of Metal Complexes*, Plenum Press, New York, 1994.
- K. S. Schanze, D. B. MacQueen, T. A. Perkins and L. A. Cabana, *Coord. Chem. Rev.*, 1993, **122**, 63.
- K. S. Schanze, L. A. Lucia, M. Cooper, K. A. Walters, H. F. Ji and O. Sabina, *J. Phys. Chem. A*, 1998, **102**, 5577.
- M. E. Walther and O. S. Wenger, *Dalton Trans.*, 2008, 6311.
- J. C. Freys and O. S. Wenger, *Eur. J. Inorg. Chem.*, 2010, 5509.
- S. Boyde, G. F. Strouse, W. E. Jones and T. J. Meyer, *J. Am. Chem. Soc.*, 1989, **111**, 7448.
- G. J. Wilson, A. Launikonis, W. H. F. Sasse and A. W. H. Mau, *J. Phys. Chem. A*, 1997, **101**, 4860.
- M. D. Ward, *Coord. Chem. Rev.*, 2006, **250**, 3128.
- R. T. F. Jukes, V. Adamo, F. Hartl, P. Belser and L. De Cola, *Coord. Chem. Rev.*, 2005, **249**, 1327.
- B. Schlicke, P. Belser, L. De Cola, E. Sabbioni and V. Balzani, *J. Am. Chem. Soc.*, 1999, **121**, 4207.
- N. J. Turro, *Molecular Photochemistry*, New York, Amsterdam, 1967.
- A. Weller, *Z. Phys. Chem. (Leipzig)*, 1982, **133**, 93.

-
- 69 G. G. Gurzadyan and S. Steenken, *Chem.–Eur. J.*, 2001, **7**, 1808.
- 70 F. D. Lewis, A. K. Thazhathveetil, T. A. Zeidan, J. Vura-Weis and M. R. Wasielewski, *J. Am. Chem. Soc.*, 2010, **132**, 444.
- 71 M. Borgström, O. Johansson, R. Lomoth, H. B. Baudin, S. Wallin, L. C. Sun, B. Åkermark and L. Hammarström, *Inorg. Chem.*, 2003, **42**, 5173.
- 72 O. S. Wenger, *Inorg. Chim. Acta*, 2011, **374**, 3.
- 73 D. Hanss, M. E. Walther and O. S. Wenger, *Coord. Chem. Rev.*, 2010, **254**, 2584.
- 74 O. Nicolet and E. Vauthey, *J. Phys. Chem. A*, 2002, **106**, 5553–5562.
- 75 M. A. Haga, E. S. Dodsworth, G. Eryavec, P. Seymour and A. B. P. Lever, *Inorg. Chem.*, 1985, **24**, 1901.